

Gas Sorption Analysis of Pore Size Distribution and Pore Anisotropy of Mesoporous Materials

Nuradeen Labaran Tanko¹ and Auwal Shehu Tijjani²

¹Department of Petroleum and Gas Engineering, Faculty of Engineering, Baze University, Plot 686, Cadastral Zone C00, Kuchigoro, Abuja, Nigeria.

²Department of Electrical and Computer Engineering, Faculty of Engineering, Baze University, Plot 686, Cadastral Zone C00, Kuchigoro, Abuja, Nigeria.
Corresponding Author: Nuradeen Labaran Tanko

Abstract : In this research, the pore anisotropy of porous media have been estimated. The methodology is based on the pore size distribution and the surface area distribution, both calculated from nitrogen adsorption and desorption isotherms. However, the original testing method by Pomonis and Armatas erred and left out some fundamental assumptions and parameters, nevertheless, the resultant analysis was satisfactory for the materials tested. The original pore anisotropy methodology has been modified and tested on porous alumina and silica materials. The materials studied are chemically pure mesoporous silica and alumina catalyst support pellets with simplified pore sizes, pore size distribution, and surface chemistry. A measure of the pore length (α) was derived from the method. Therefore, pore anisotropy estimation method has severe limitations due to the inability to measure pore length of the samples. Nevertheless, samples with very positive slope (α) would have long pores depending on the size of the constant in the power law correlation. These values are in the range of 5.055 ± 0.520 to 1.514 ± 0.140 , respectively.

Keywords -Porous Media, Gas adsorption, Porosimetry, Pore anisotropy

Date of Submission: 05-03-2018

Date of acceptance: 19-03-2018

I. Introduction

The measurement of pore size, geometry, and interconnectivity of mesopores and macropores in porous materials continues to be an important activity in oil and catalyst industries. The term “porosimetry” is often used to encompass the measurements of pore size, pore volume, pore size distribution, and other porosity-related characteristics of a porous material. Gas sorption and mercury porosimetry are complementary methods with the latter covering a much wider size range (0.0035 to 500 μ m). There are well-known and standard techniques from gas sorption that can determine key characteristic parameters of porous media, such as the pore size according to the Kelvin Equation [1], pore volume and BET surface area [2], BJH algorithm for pore size distribution [3], and pore connectivity by percolation analysis [4]. Therefore, these established methods from gas sorption and percolation theory have been widely used, however, pore length and pore length distribution is yet to be fully understood. Although it was found by [5] from various micro-photographic images of solids with random porosity that in many cases the length (l) of pores is very close to their diameter (d) of the pores ($l \approx d$). In this regard, the measure of pore length and its respective distribution will inveterately elucidate our understanding of rate of mass transport processes in porous solid.

In this regard, [6] presented an analytical method to determine the pore-length distribution from the results of novel experiments using the integrated nitrogen sorption and mercury porosimetry techniques. These researchers analysed two sets of nitrogen sorption data, taken from integrated nitrogen sorption and mercury porosimetry experiments to derive the pore-length distribution by using the percolation theory developed by [4]. As in the original percolation method by [4], the analysis presented by [6] was carried out in terms of percolation variables, the values of which were calculated from pore-diameter distributions (obtained from nitrogen adsorption isotherms). In the old version of [4] percolation theory, it was assumed that the average pore length is independent of pore diameter. Consequently, [6] assumed that the average pore length of pores is a function of the pore diameter, such that the distribution of average pore length for each pore diameter follows a power law.

In a different approach to the work of [6-7], proposed a method for the estimation of pore anisotropy in porous solids. The methodology is based on the pore size distribution and the surface area distribution, both calculated from nitrogen adsorption and desorption isotherms. The materials used for original testing of the method were aluminium containing Mobil crystalline materials (MCM) and silicas with different random porosity. However, [7] erred and thus left some important assumptions and parameters out of the correlation in

their methodology that will be discussed later in Section II. Nevertheless, the resultant analysis was satisfactory for the materials they tested.

The objective of this research is to improve the research of [7]. The research will be applied to several mesoporous materials with the aid of gas adsorption porosimetry to check its general applicability. In addition, for related analysis, gas sorption would be used to determine key characteristic permeability parameters such as the BET surface area, Pore Size, and pore size distribution. Furthermore, the work of [5] would be tested experimentally where it was hypothesised that from various micro-photographic images of solids with random porosity that in many cases the length (l) of pores is very close to their diameter (d) of the pores ($l \approx d$).

II. Theory

Adsorption pore size distribution analysis of mesoporous materials is based on an adopted interpretation of the mechanisms of capillary condensation, evaporation and the associated hysteresis phenomena [8]. The theory for condensation of vapour into a porous medium is derived from thermodynamic considerations. This is known as the Kelvin Equation given by:

$$RT \ln x = \frac{-2\gamma_{LV}V_L \cos\theta}{r_k} \quad (1)$$

Where $R, T, x, \gamma_{LV}, V_L$ and r_k are universal gas constant, temperature, relative pressure, interfacial surface tension between liquid, molar volume and vapour and radius of condensate with a meniscus of hemispherical form.

Within a porous material, the gas layers continue to fill the pore until the pressure is sufficient that the gas condenses into a 'liquid-like phase'. The pressure at which the gas condenses can be related to the pore size according to the Kelvin equation. However, it becomes less accurate as the PSD becomes smaller because the Kelvin equation is purely thermodynamic, and thus, it does not take account at micropore region [4]. This model is usually applied for diameters greater than 2 nm, because below this size the liquid cannot be considered a fluid with bulk properties due to forces exerted by the pore wall. Theoretical calculations suggest that the properties of fluids in microporous structures are highly sensitive to the size of the pores [9].

In the case of mesopores, (1) provides a useful model for the transformation of adsorption data into a PSD [9]. There established algorithms based on (1) that are used for the determination of PSD such as the Barrett Joyner and Halenda (BJH) method by [3]. However, there are other approaches that consider the fluid-solid interactions. The Horvath-Kawazoe (HK) method is a novel technique for determining the micropore size distribution. The method was originally used to analyse nitrogen adsorption on molecular sieve carbons with slit shaped pores but has since been modified to account for cylindrical shaped pores as in the case of silica mesopores. The HK method is based on the general idea that the relative pressure required for the filling of micropores of a given shape and size, is directly related to the adsorbent-adsorbate interaction energy. Nevertheless, the BJH method is undoubtedly the most widely accepted method for the analysis of nitrogen adsorption/desorption PSD and thus, it has been adopted in this investigation [9].

When the BJH algorithm is used to determine the PSD, the pore size obtained from (1) is generally corrected for the multi-layer film thickness using a universal t -layer equation. The empirical observation have shown that, for many non-porous surfaces, the ratio of the volume adsorbed to the monolayer capacity plotted against relative pressure all approximately fit a common Type II curve above a relative pressure of 0.3. This implies for a given value of the adsorbed layer thickness will be the same regardless of the adsorbent. However, the data used to compile common-curves was not comprehensive and the universality was only approximated [10]. Therefore, an individual porous solid may show a deviation from the common t -curves, as observed experimentally for nonporous templated silicas, such as the SBA-15 using neutron scattering [11].

In [7] proposed a method for the estimation of pore anisotropy, b , in porous solids. This method is based on the pore size distribution and the surface area distribution, both calculated from nitrogen adsorption and desorption isotherms. The materials used for original testing of the method were aluminium containing Mobil crystalline materials (MCM) and silicas with different random porosity. In a similar approach, [11] used [7, 12] method to estimate anisotropy in Nano structured mesoporous solids. Other researchers that used [7, 12] include but not limited to [13-14]. However, [7, 12] left out some important assumptions and parameters out of the correlation in their methodology that will be discussed later in this section. Nevertheless, the resultant analysis for the aforementioned researchers was satisfactory for the materials tested.

In furtherance of our stated objective in Section I, we proceed based on the assumption by [7] collection of pores, for each pore (i), or rather for each group of pores in a small interval of pore diameter ($d_i \pm \Delta d_i$), the length (l), is related to the diameter (d_i), via (2):

$$b_i = \frac{l_i}{d_i} = \frac{l_i}{2r_i} \tag{2}$$

If (b_i) is larger than unity, those pores have a large anisotropy. Whilst, if ($b_i \approx 1$), the pores are isotropic and should be the case in ordinary porous solids with a random porous network. However, if on the other hand (b_i) smaller than unity, the pores are again anisotropic but assumed to be shallow cavities rather than typical pores.

From the gas sorption experiments, we can calculate at each $P_i \left(\frac{P_i}{P_0} \right)$ the values corresponding to specific pore surface area S_{pi} and the specific pore volume V_{pi} . At each P_i we assume that a number N_i of cylindrical pores is filled up. Furthermore, [7] assumed that:

$$S_{pi} = N_i (2\pi r_i) l_i = N_i (2\pi r_i) (2b_i r_i) = 4\pi N_i b_i r_i^2 \tag{3}$$

And

$$V_{pi} = N_i (\pi r_i^2) l_i = N_i (\pi r_i^2) (2b_i r_i) = 2\pi N_i b_i r_i^3 \tag{4}$$

Thus, dividing the cube of (3) and the square of (4) gives the dimensionless ratio:

$$\frac{S_i^3}{V_i^2} = \frac{N_i 8\pi^3 r_i}{r_i} \tag{5}$$

Substituting (2) into (5) will give the ratio of the cube of surface area S_i over the square of pore volume V_i , at each particular pressure as:

$$\frac{S_i^3}{V_i^2} = 16\pi (N_i b_i) = 16\pi \lambda_i \tag{6}$$

Where $N_i b_i$ is the number of pores having anisotropy b_i , which are filled at each pressure $\left(\frac{P_i}{P_0} \right)$ and λ_i is the total anisotropy of all the pores N_i belonging to the group i of pores. Therefore, the plot of λ_i against $\left(\frac{P_i}{P_0} \right)$ provides a clear picture of the variation of the total pore anisotropy λ_i as the relative pressure $\left(\frac{P_i}{P_0} \right)$ increases. It

should be noted that N_i and b_i are constants. The particular values of N_i and b_i can be obtained by using the power law correlation:

$$l_i = k r_i^{\alpha_i} \tag{7}$$

Note that [7] missed out the all-important proportionality constant k (in grams) in the power law correlation (7). Finally, substituting (6) into (7) gives:

$$\frac{S_i^3}{V_i^2} = N_i 8\pi k^{\alpha_i - 1} \tag{8}$$

Taking the logarithm of (8) gives:

$$\log \left(\frac{S_i^3}{V_i^2} \right) = \log(8\pi k) + \log(N_i) + [(\alpha_i - 1) \times \log r] \tag{9}$$

A plot of $\log\left(\frac{S^3}{V^2}\right)$ against $\log(r_i)$ should give rise to a line with slope $s_i = \alpha_i - 1$.

Note that [7] left out the important assumption for (9) to be valid for a straight line. As result, can only be a straight line if α_i and N_i are constant for all d_i . The slope at each point i of the plot is equal to $s_i = \alpha_i - 1$ since:

$$l_i = b_i d_i = 2r_i b_i = kr_i^{\alpha_i - 1} \tag{10}$$

Therefore:

$$b_i = 0.5kr_i^{\alpha_i - 1} = 0.5k_i s_i \tag{11}$$

In a subsequent report, [11] expanded the work of [7] by applying the model to nanostructured ordered mesoporous solids. These researchers succeeded in estimating not only the anisotropy of pores in a mesoporous solid but also the related pore anisotropy distribution (PAD). The model to nanostructured mesoporous silicate materials was tested by [14]. However, as seen in the power correlation (7), the pore anisotropy with corresponding PAD cannot be obtained, and thus, the work of [11] and [14] can be considered incorrect. In [7] the method can only determine the slope of the (9), which can tell some measure of the average pore length and perhaps the heterogeneity of the sample.

III. Experimentation

3.1 Material

The material studied in this work is a commercially available, chemically pure mesoporous silica and alumina catalyst support pellet with simplified pore sizes, pore size distribution, and surface chemistry. As highlighted in Table 1, the materials have pore size lying in the range of 7-30 nm. The majority of the materials have unimodal structure with the exception of one bimodal structured material (AL3984T).

Table 1: A range of alumina and Silica materials tested

S/N	Sample	Material	Pellet form	Voidage	Nominal diameter (mm)
1	Aerosil	Silica (SiO ₂)	Fumed sphere	N/D ^{a*}	3.5
2	AL3984T	Alumina (Al ₂ O ₃)	Tablet	0.59	3.0
3	AL3992E	Alumina (Al ₂ O ₃)	Extrudate	0.65	3.0
4	C10	Silica (SiO ₂)	Gel sphere	0.66	3.0
5	C30	Silica (SiO ₂)	Gel sphere	0.69	3.0
6	P7129	Silica (SiO ₂)	Gel sphere	0.67	3.0
7	Q17/6	Silica (SiO ₂)	Gel sphere	0.49	3.5
8	S980A	Silica (SiO ₂)	Gel sphere	0.6	3.0
9	S980G	Silica (SiO ₂)	Gel sphere	0.61	2.2
10	Silica Alumina	Silica and Alumina (Al ₂ O ₃ Si)	Extrudate	0.60	0.5

Note: a* – Not detected

3.2 Gas sorption porosimeter and experimental consideration

On each sample, nitrogen sorption experiment was carried out at 77K using a micromeritics accelerated surface area porosimeter (ASAP) 2010 apparatus. Initially, about 0.2 g of the sample was left under vacuum for 4 hours at a pressure of 0.27 Pa as recommended by [17]. The purpose of the thermal pre-treatment for each sample was to drive any physisorbed water on the sample while leaving the morphology of the sample itself unchanged. The sample tube and its contents were then re-weighed after cooling to room temperature. Thus, the dry weight of the sample before being transferred to the analysis port for the automated analysis procedure was measured. In the case of mesopores, the Kelvin Equation provides a useful model for the transformation of adsorption data into a PSD [18] and thus, it has been adopted in this study. The adsorbate property factor was taken as 9.53×10^{-10} m. Furthermore, it was assumed that, the fraction of pores open at both ends was zero, for both adsorption and desorption. Thus, capillary condensation commenced at the closed end of a pore to form a hemispherical meniscus, and the process of evaporation commenced at a hemispherical meniscus. A full adsorption/desorption micro/mesoporous was carried out since the samples' characteristics are unknown.

The calculation of the dead volume of flask (free space analysis) was carried out by using helium. The dead space was the volume of the sample tube excluding the sample itself. As also recommended by [17], equilibration time for the diffusion of nitrogen molecules to access most of the pores present in these materials was set at forty-five seconds.

IV. Result and Analysis

In order to allow for the variation of support structure between pellets from the same batch and to test the reproducibility of measurements, replicate measurements are used. Sets 1 and 2 represent the replicate measurements, respectively. Therefore, the reported parameters in this section are the mean of the sets used. Also, during the course of experiments, the relative pressure was either increased or decreased in small steps, and a small volume of nitrogen, either enters, or leaves the sample. In this study, the method of estimating pore length proposed by [7] was corrected in Section II and tested in all samples. As detailed Section II, the method cannot be used to determine the pore length. However, it can be used to determine a parameter (α) which demonstrates the degree of pore length. This parameter can be determined directly from the slope ($\alpha - 1$) of (9).

Thus, according to (9), the plot of $\log\left(\frac{S^3}{V^2}\right)$ against $\log(r_i)$ provides a line, with slope ($\alpha - 1$), and intercept

$8\lambda kN$. It can be seen in Fig. 1 to 8, the plots in this study are suitable for the following pore size range, 6.485 - 106.18 nm. A respectable degree of linearity was obtained for these plots. For general simplification, a coefficient of determination (R^2) ≥ 0.95 has been adopted for the analysis of the slope ($\alpha - 1$) values. The highlights of the key findings are presented in Table 2. The reported uncertainties in Table 2 indicate the spread of the results over samples from the same batch, and the error associated with the technique. It can be seen in Table 2 that the slope ($\alpha - 1$) for samples is negative with the exception of C30 and S980G.

Table 2: The average anisotropy

Sample	Pore size range (nm)		Coefficient of determination, R^2		Slope ($\alpha-1$)		Intercept ($8\lambda kN$)	
	Set 1	Set 2	Set 1	Set 2	Set 1	Set 2	Set 1	Set 2
Aerosil	6.485-06.18	6.485-106.18	0.983	0.958	-3.855±0.260	-3.824±0.4	21.44±0.32	21.51±0.48
AL3984T	6.26-29.05	6.385-31.62	0.956	0.959	-4.069±0.440	-5.055±0.52	20.68±0.48	22.32±0.59
AL3992E	N/S	N/S	N/S	N/S	N/S	N/S	N/S	N/S
C10	N/S	0.86-5.95	N/S	0.970	N/S	-2.059±0.08	N/S	19.77±0.03
C30*	N/S	5.805-26.89	N/S	0.975	N/S	1.249±0.12	N/S	15.6±0.13
Q17/6	6.33-27.18	N/S	0.965	N/S	-4.635±0.440	N/S	22.22±0.48	N/S
S980A	N/S	0.09-0.45	N/A	0.980	N/S	-0.29±0.01	N/S	18.63±0.01
S980G*	N/S	6.405-29.43	N/A	0.965	N/S	1.514±0.14	N/S	14.47±0.2
Silica Alumina	0.545-3.08	6.805-120.13	0.978	0.966	-4.609±0.310	-3.641±0.31	17.21±0.08	20.83±0.41

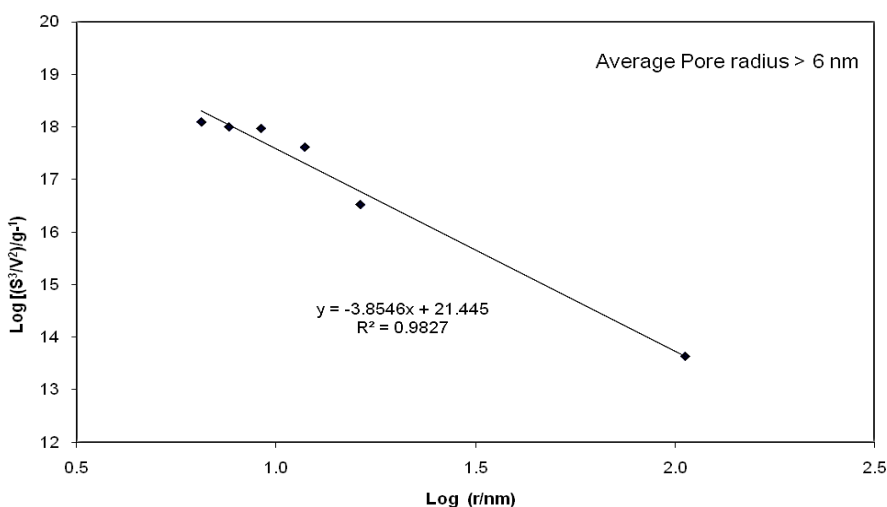


Fig. 1: Variation of the parameter $\log(\lambda_i)$ as a function of pore radius $\log(r_i)$ for Aerosil

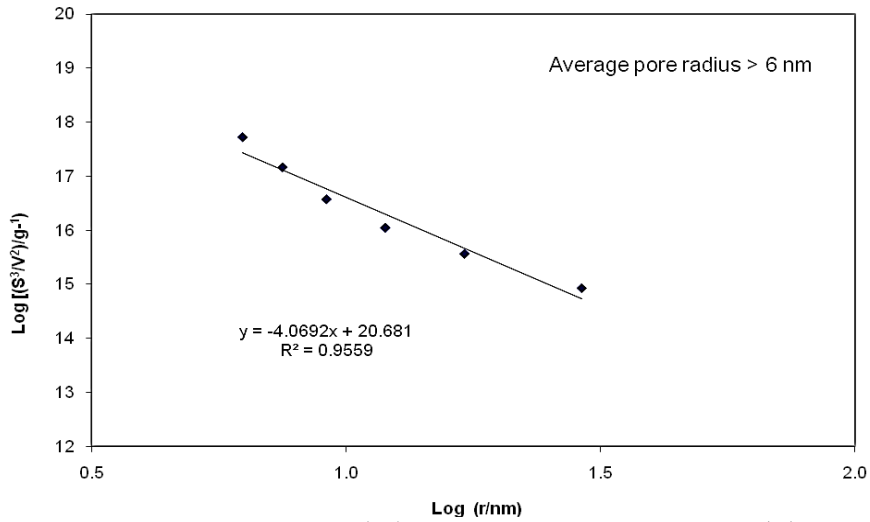


Fig. 2: Variation of the parameter $\log(\lambda_i)$ as a function of pore radius $\log(r_i)$ for AL3984T

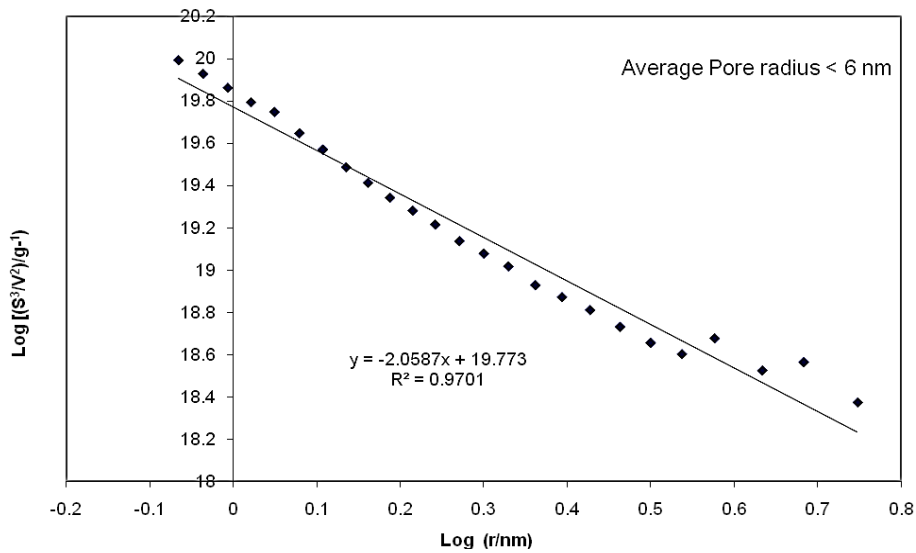


Fig. 3: Variation of the parameter $\log(\lambda_i)$ as a function of pore radius $\log(r_i)$ for C10

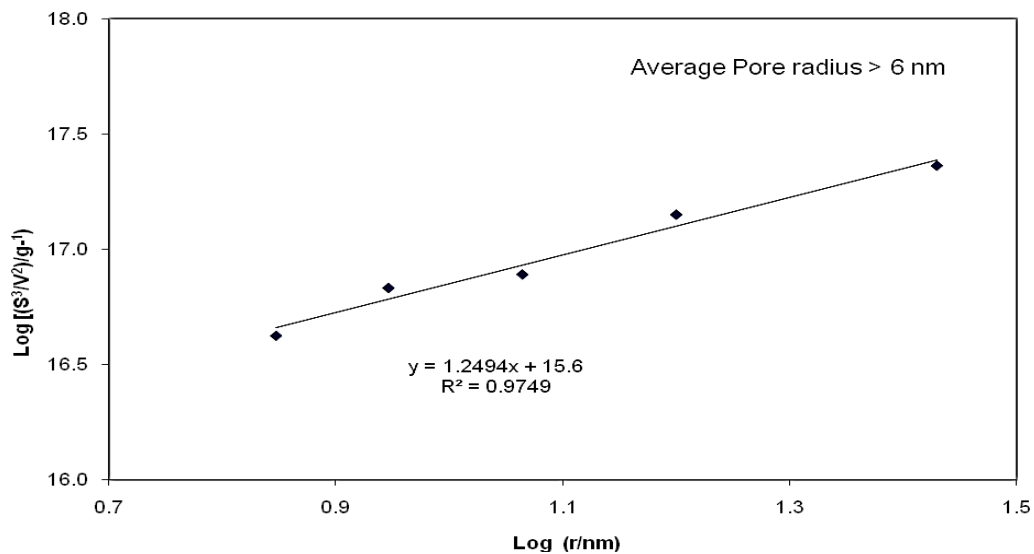


Fig. 4: Variation of the parameter $\log(\lambda_i)$ as a function of pore radius $\log(r_i)$ for C30

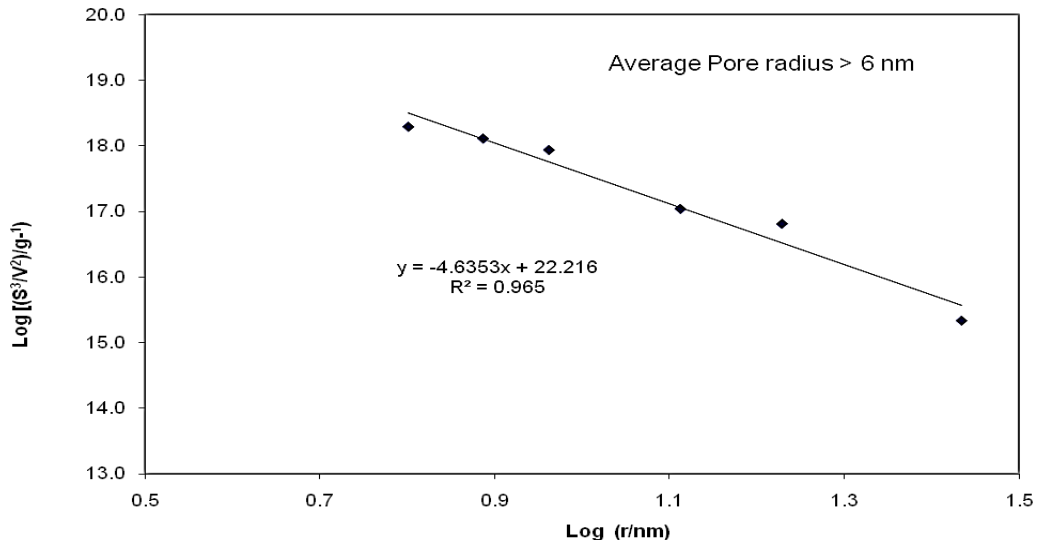


Fig. 5: Variation of the parameter $\log(\lambda_i)$ as a function of pore radius $\log(r_i)$ for Q17/6

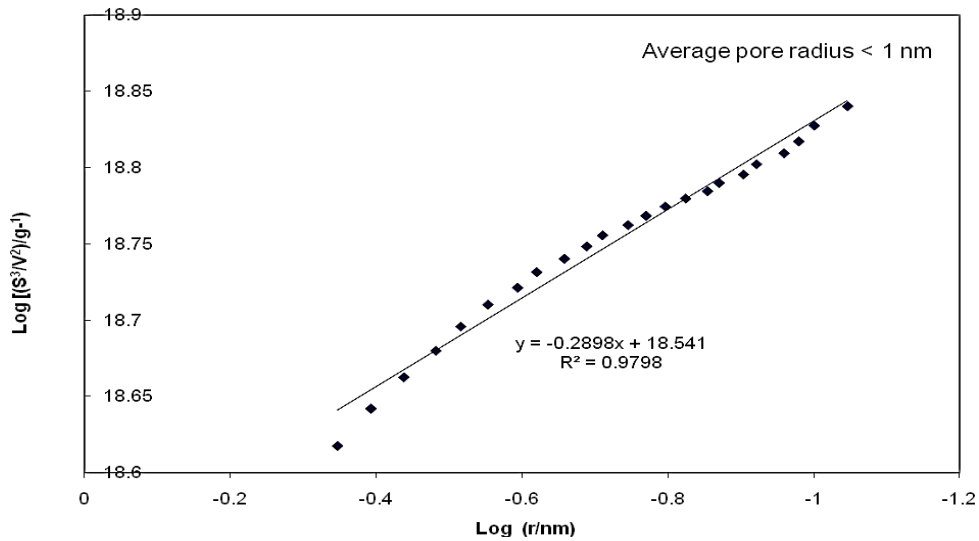


Fig. 6: Variation of the parameter $\log(\lambda_i)$ as a function of pore radius $\log(r_i)$ for S980A

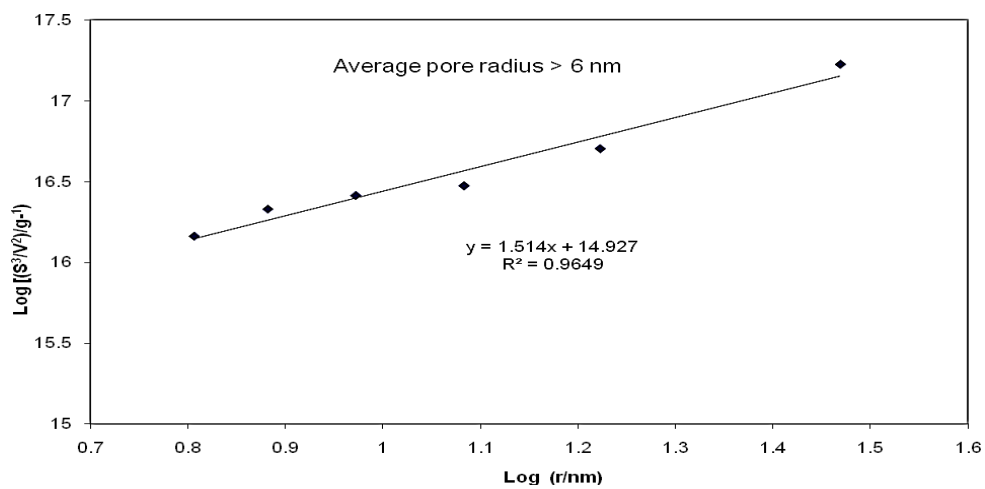


Fig. 7: Variation of the parameter $\log(\lambda_i)$ as a function of pore radius $\log(r_i)$ for S980G

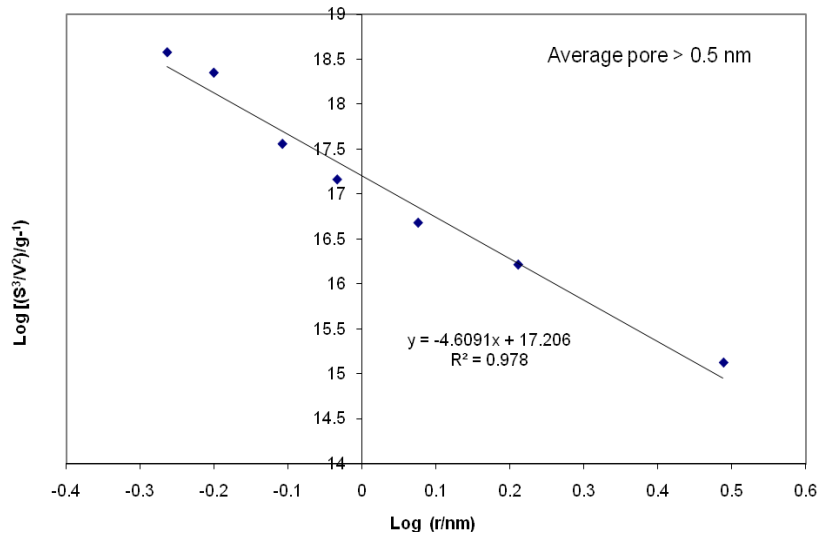


Fig. 8: Variation of the parameter $\log(\lambda_i)$ as a function of pore radius $\log(r_i)$ for Silica Alumina

V. Discussion

In [7] the method of estimating the pore anisotropy b , in porous solids was developed and tested on MCM materials. These MCM materials generally have long cylindrical pores with well-defined length and diameter [15]. In contrast, the materials in this study are generally associated with a random pore network, and thus it is difficult to measure the cylindrical geometrical parameters. However, it was seen in several microphotographic images that traditional porous materials such as the silica and alumina have pores with diameters that are nearly close to their length [5]. In addition, various observations made by electron microscopy have shown that many traditional porous materials appear to be random collection of packed spherical and semi-spherical particles as well as cylinders [16]. Therefore, it is safe to suggest that the method proposed by [7] is suitable for the estimation of pore length parameter (α) used in this research. In point of fact, it was successfully tested on the materials. The BJH adsorption algorithm was used to obtain the PSD of the materials.

The plot of $\log\left(\frac{S^3}{V^2}\right)$ against $\log(r_i)$ produced a straight line with a slope $(\alpha - 1)$ and intercept

$87kN$.

In general, the plots worked reasonably well for a particular pore size range (6.485 - 106.18 nm). However, as detailed in Section II, the method cannot be used to estimate the pore anisotropy, b , in porous solids, and thus the pore-length cannot be determined from the power law correlation (10). The failure of the method to estimate the pore anisotropy, b , is due to the fact that, the intercept $87kN$ has an unknown parameter k . The unknown parameter k (in grams) is from the power law correlation (10). In [6] similar problems with power law correlations was encountered. The typical pore lengths obtained were of the order of several micrometres. These researchers thought the values were unrealistically large for a single mesopore in an amorphous material. Therefore, it is safe to connect the failure for estimating pore length of these materials from nitrogen sorption data to the power law correlation. However, the pore length parameter (α) obtained from the power law can be used for the pore length analysis. It can be seen in Table 2.0 that the pore length parameter (α) obtained for the silica materials is close to or greater than zero. The manufacturing conditions of silica materials make them heterogeneous with different pore shapes and wide pore size distributions. Therefore, these materials might have a combination of several long cylindrical pores and ink bottle pores. For example, the pore length parameter (α) of C30 and S980G are 2.249 and 2.514, respectively. By using the power correlation (10), it can be said that these samples would have long pores depending on the size of k (in grams). In [5] similar findings in samples with random porous network with $b_i \sim 1 (l_i \sim d_i)$, was investigated and thus, the pores were assumed to be isotropic. In contrast, [5] observed shallow cavities rather than typical pores in samples with random porous network with $b_i < 1$. For example, the pore length parameter (α) of AL3984T is -4.055. By using the power correlation (10), it can be said that this sample would have short pores depending on the size of k . The manufacturing conditions of Alumina materials results in a well-defined pore structure forms, and thus,

alumina materials are less heterogeneous than silica materials. Finally, it can be concluded that the pore length parameter (α) is sensitive to the method of production of the materials. Heterogeneous samples such as C30 and S980G have big positive values. In contrast, the alumina materials such as AL3984T have a very negative slope. Therefore, it is safe to deduce that pore length parameter (α) is suitable for measuring the heterogeneity of porous materials such as the silica and alumina materials investigated in this study.

VI. Conclusion

Gas adsorption studies carried out on all samples revealed isotherms of type IV classification, according to the IUPAC, which is typical of the monolayer–multilayer coverage to capillary condensation pattern, with reproducible type H2 hysteresis loops. In general, the Type H2 hysteresis loop has been traditionally ascribed to a collection of ink-bottle type pores which are susceptible to pore-blocking phenomena. Most of the samples have strong interactions between the adsorbate and adsorbent, and thus are susceptible to advanced condensation phenomena that will result in a narrower PSD than exists in reality. In contrast, a consideration of the method of estimating pore length proposed by [7] suggested had severe limitations due to the inability to measure pore length of the samples. Nevertheless, a measure of the pore length was derived from the method. It was concluded that samples with very positive slope would have long pores depending on the size of the constant in the power law correlation.

References

- [1] Thomson, S.W., On the equilibrium of vapour at a curved surface of liquid. The London, Edinburgh and Dublin Philosophical Magazine and Journal of Science, series 4, 42 (282): 448–452.
- [2] Brunauer, S., Emmett, P. H., and Teller, E., Adsorption of Gases in Multimolecular Layers, Journal of the American Chemical Society, 60, 1938, 309-319.
- [3] Barrett, E. P., Joyner, L. G., Halenda, P. P., The determination of pore volume and area distributions in porous substances. I. Computations from nitrogen isotherms, J. Am. Chem. Soc., 73, 1951. 373–380.
- [4] Seaton, N.A., Determination of the connectivity of porous solids from nitrogen sorption measurements. Chemical engineering science, 46 (8), 1999, 1895-1909.
- [5] Dullien, F.A.L., In porous media; Fluid transport and pore structure. New York: Academic press. 2nd edition. 1992.
- [6] Rigby, S.P., Watt-Smith, M.J., Fletcher, R. S., Simultaneous determination of the pore-length distribution and pore connectivity for porous catalyst supports using integrated nitrogen sorption and mercury porosimetry. Journal of catalysis, 227 (1), 2004, 68-76.
- [7] Pomonis, P.J., and Armatas, G.S., A method of estimation of pore anisotropy in porous solids. Langmuir, 20, 2004, 6719-6726.
- [8] Sing, K.S.W., Everett, D.H., Haul, R.A.W., Moscou, L., Pierotti, R.A., Rouquerol, J. and Siemieniewska, T., Reporting physisorption data for gas solids systems with special reference to the determination of surface area porosimetry and porosity, Pure and applied chemistry, 57, 1985, 603-619.
- [9] Rouquerol, F., Rouquerol, J., and Sing, K., Adsorption By Powders And Porous Solids Principles, Methodology And Applications. London: Academic Press, 1999.
- [10] Rigby, S.P., Gladden, L.F., The use of magnetic resonance images in the simulation of diffusion in porous catalyst support pellets. Journal of Catalysis, 173 (2), 1998, 484-489.
- [11] Knowles, J., Armatas, G., Hudson, M., Pomonis, P.J., Pore Anisotropy and Microporosity in Nanostructured Mesoporous Solids. Langmuir, 22 (1), 2006, pp 410–418.
- [12] Pomonis, P.J., and Margellou, A., Zipf's law for pore ranking and pore anisotropy. Physical Chemistry Chemical Physics. Issue 26, 2017.
- [13] Margellou, A., and Pomonis, P.J., The total and the differential mean pore anisotropy in porous solids and the ranking of pores according to Zipf's law. Physical Chemistry Chemical Physics. Issue 2, 2017.
- [14] Katsoulidis, A.P., Petrakis, D.E., Armatas, G.S., Pomonis, P.J., Microporosity, pore anisotropy and surface properties of organized mesoporous silicates (OMSi) containing cobalt and cerium. Journal of Materials Chemistry. Issue 15, 2007.
- [15] Kresge, C.T., Leonowicz, M.E., Roth, W.J., Vartuli, J.C., Beck, J.S., Ordered mesoporous molecular sieves synthesized by a liquid crystal template mechanism. Nature, 359, 1992, 710-712.
- [16] Drewry, H. P. G., and Seaton, N. A., Continuum random walk simulations of diffusion and reaction in catalyst particles. AIChE Journal, 41, 1995. 880–893.
- [17] Egbuomwan, O.E., The structural characterisation of porous media for use as a model reservoir rocks, adsorbents and catalyst. Thesis (PhD). University of Bath, 2009.
- [18] Ravikovitch, P. I., and Neimark, A. V., Experimental confirmation of different mechanisms of evaporation from Ink bottle type Pores: equilibrium, pore blocking and cavitation, Langmuir, 18, 2002, 9830-9837.

Nuradeen Labaran Tanko "Gas Sorption Analysis of Pore Size Distribution and Pore Anisotropy of Mesoporous Materials." IOSR Journal of Applied Geology and Geophysics (IOSR-JAGG) 6.2 (2018): 28-36.